PROCEEDINGS A

rspa.royalsocietypublishing.org

Research

Cite this article: Nassar H, Chen YY, Huang GL. 2018 A degenerate polar lattice for cloaking in full two-dimensional elastodynamics and statics. *Proc. R. Soc. A* **474**: 20180523. http://dx.doi.org/10.1098/rspa.2018.0523

Received: 3 August 2018
Accepted: 18 October 2018

Subject Areas:
mechanical engineering, wave motion

Keywords:
cloaking, transformation method, minor symmetry, form invariance, pentamode materials, homogenization

Author for correspondence:
G. L. Huang
e-mail: huangg@missouri.edu

A degenerate polar lattice for cloaking in full two-dimensional elastodynamics and statics

H. Nassar, Y. Y. Chen and G. L. Huang

Department of Mechanical and Aerospace Engineering, University of Missouri, Columbia, MO 65201, USA

HN, 0000-0001-7235-4498; GLH, 0000-0002-6238-6127

A lattice design of a cloak for full two-dimensional elasticity is suggested when the background continuum is isotropic with Lamé parameters (λ, μ) satisfying $\mu \leq \lambda$. The lattice is *polar* in the sense that it elastically resists rotations; and is *degenerate* meaning it admits a stressless collapse mechanism. These characteristics are attained through the use of appropriately distributed restoring torques in conjunction with hinge-like spring-mass contacts. Thus, the lattice is proven to exhibit a rank-3 elasticity tensor lacking the minor symmetries. Accordingly, it rigorously adheres to the form-invariance requirements of the transformation method under the Brun–Guenneau–Movchan gauge. The cloak is numerically tested in statics and in dynamics under pressure and shear incident waves and shows satisfactory performance. Finally, a theoretical generalization extends the design to three dimensions and to arbitrarily anisotropic backgrounds so as to enable cloaking as well as other transformation-based static and dynamic field manipulation techniques in these cases.

1. Introduction

An elastic cloak is a coating that can be applied to an arbitrary inclusion to make it indistinguishable from the background medium. The coated inclusion becomes undetectable by elastographic techniques, be they static or dynamic. To determine the material the coating is made of, one applies a curvilinear change of coordinates given by a singular geometric transformation that (i) blows-up a point of the background into the inclusion; and (ii) does not disturb the background

THE ROYAL SOCIETY PUBLISHING

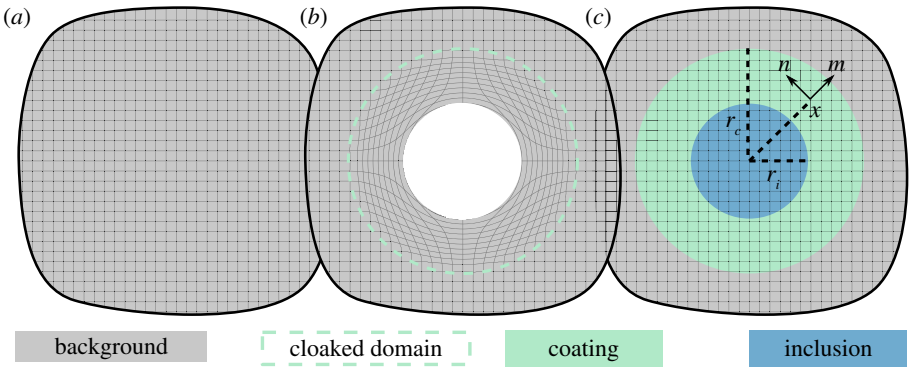

Figure 1. The transformation method: (*a*) background medium described by Cartesian coordinates **X**; (*b*) background medium described by curvilinear coordinates $\mathbf{x} = \boldsymbol{\phi}(\mathbf{X})$; (*c*) Reinterpreting **x** as Cartesian coordinates makes appear a gradient of constitutive properties (in green). Here, the illustrated transformation blows-up a point from (*a*) into a disc (in white) on (*b*) without disturbing the region falling beyond some horizon (in dashed lines) and is suitable for cloaking purposes. The disc, having a scattering cross section equal to that of a point, can be filled with any inclusion without disturbing the fields beyond the horizon. (Online version in colour.)

beyond a horizon outlining the boundary of the cloak; see, e.g. figure 1 and other examples by Hu *et al.* [1]. The constitutive parameters of the cloaking material can then be read from the equations of elasticity written in the new coordinates. This design method, known as the transformation method, was first discovered for conductivity by Greenleaf *et al.* [2,3], then for geometric optics by Leonhardt [4] and for electromagnetism by Pendry *et al.* [5] and later applied to acoustics by others [6–8].

In all of these cases, when the background medium is isotropic, the coating turns out to be anisotropic. To design anisotropic coatings can be particularly challenging and yet ultimately proved feasible. Norris [9] showed how to design an anisotropic acoustic medium for instance; see also Smith [10]. By contrast, the coating necessary for elastic cloaking is not only anisotropic but also exhibits a non-standard constitutive behaviour whose exact nature depends on the gauge of the adopted transformation. The Milton–Briane–Willis (MBW) gauge, after Milton *et al.* [11], requires the transformed stress to be symmetric and makes an unusual stress-displacement coupling appear. The Brun–Guenneau–Movchan (BGM) gauge, after Brun *et al.* [12], requires displacements to be identical before and after transformation and makes elasticity tensors with broken minor symmetries appear; see also Diatta & Guenneau [13]. More general gauges investigated by Norris & Shuvalov [14] are shown to mix both effects and, as of yet, there are no known elastic materials that could play the role of coating in any gauge.

That is not to say that elastic cloaking is non-existent. Several successful attempts have indeed been made to demonstrate various degrees of elastic cloaking in a number of important special cases. For reference, Farhat *et al.* [15–17], Stenger *et al.* [18], Brun *et al.* [19] and Colquitt *et al.* [20] designed and tested cloaks for bending waves in thin plates; see also the active control strategy by Chen *et al.* [21]. Parnell *et al.* [22], Parnell [23] and Norris & Parnell [24] employed prestressed hyperelastic materials to cloak against antiplane and inplane elastic waves. Bückmann *et al.* [25] designed an approximate cloak in a hexagonal lattice and tested it under uniaxial static compression and Sklan *et al.* [26] approximately shielded a tunnel against incident pressure and shear waves. Not to mention the existence of an extensive literature dealing with neutral inclusions where a specific inclusion is cloaked against a specific loading but where cloaking fails when either inclusion or loading changes; see Milton [27] for further references.

Among these, the work of Norris & Parnell [24] stands out. It is the only one to adhere to the transformation method in its full form rigorously. In comparison, the other contributions, one way or another, discarded altogether the tensorial character of elasticity in favour of a scalar

theory. While this attitude is natural in some cases, as in bending of plates or in acoustics, it is hardly justifiable in other cases. Unfortunately, Norris & Parnell [24] revealed that their approach requires the blow-up ratio, the one transforming figure 1*a* into *b*, to be smaller than two. This means that their prestressed hyperelastic materials can only substitute the cloak near its outer boundary. At the inner boundary, their approach fails as the blow-up ratio nears infinity. In practical terms, their design reduces scattering of inplane waves without achieving perfect cloaking.

The main purpose of the paper is to suggest a lattice cloak for full two-dimensional elastodynamics and statics. By a scrutiny of the transformation method, we demonstrate that such a lattice is necessarily *polar* in that it elastically resists rotations; and *degenerate* in that it admits a stressless collapse mechanism. Both requirements are then satisfied through the use of appropriately distributed torques and hinge-like spring-mass contacts. Thus, the designed lattice is proven to exhibit a rank-3 elasticity tensor lacking the minor symmetries in a way that rigorously fulfills the form-invariance requirements of the BGM gauge over the complete domain of the cloak. A stability analysis shows that the design is valid when the background is isotropic with a Lamé pair (λ, μ) satisfying $\mu \leq \lambda$. Last, the cloak's performance is assessed numerically and found to be satisfactory under exhaustive static/dynamic and pressure/shear loadings.

As a theoretical generalization, we construct lattice materials which render the set of elastic materials invariant by arbitrary transformations under the BGM gauge so as to enable cloaking as well as other static and dynamic field manipulation techinques in three dimensions and in the presence of a possibly anisotropic background medium. Essential to this endeavour is an adaptation of Milton & Cherkaev's [28] pentamode materials. Thus, by mixing appropriately modified pentamode materials submitted to distributed torques, we show that all non-negative elasticity tensors with major symmetry and with or without the minor symmetries can be constructed. We stress that Guevara Vasquez *et al.* [29] similarly observed that transformation elasticity under the BGM gauge is possible in lattices featuring 'torque springs' with non-central forces; our insight is equivalent to theirs.

The remainder of the paper goes as follows. In the second section, our design of a two-dimensional cloak is investigated, the effective behaviour of the underlying degenerate polar lattice calculated and shown rigorously to match that required by the transformation method. Numerical simulations of cloaking in statics and dynamics are then presented and analysed. In the third section, a generalization to higher dimensions and arbitrary background media is carried out. Finally, we conclude with a number of remarks and comments.

2. Cloaking in full two-dimensional elasticity

Hereafter, we briefly recall how the elasticity equations transform in the BGM gauge and analyse the nature of the elasticity tensors that emerge as an outcome. A degenerate polar lattice whose behaviour can match that of a perfect two-dimensional cloak is introduced and its effective elasticity tensor calculated. Once the relevant geometric and constitutive parameters have been identified, the cloak's performance is assessed based on an exhaustive set of numerical tests in static and dynamic regimes.

(a) Transformation elasticity

We begin by analysing the constitutive behaviour of the transformed/coating material in the BGM gauge. Let

$$L(\boldsymbol{\nabla}\mathbf{U}, \dot{\mathbf{U}}) = \frac{\boldsymbol{\nabla}\mathbf{U} \cdot \mathbf{C}\boldsymbol{\nabla}\mathbf{U} - \dot{\mathbf{U}} \cdot R\dot{\mathbf{U}}}{2}, \tag{2.1}$$

be the Lagrangian density of an elastic domain $\{\mathbf{X}\}$ of elasticity tensor $\mathbf{C}$ and mass density R written as a function of displacement gradient $\boldsymbol{\nabla}\mathbf{U}$ and velocity $\dot{\mathbf{U}}$. Then, in the transformed

domain $\{\mathbf{x}=\boldsymbol{\phi}(\mathbf{X})\}$, the Lagrangian density reads

$$\ell(\boldsymbol{\nabla}\mathbf{u},\dot{\mathbf{u}})=\frac{1}{J}L(\boldsymbol{\nabla}\mathbf{u}\mathbf{F},\dot{\mathbf{u}})=\frac{\boldsymbol{\nabla}\mathbf{u}\cdot\mathbf{c}\boldsymbol{\nabla}\mathbf{u}-\dot{\mathbf{u}}\cdot\rho\dot{\mathbf{u}}}{2}, \tag{2.2}$$

where $\mathbf{F}=\partial\mathbf{x}/\partial\mathbf{X}$ is the transformation gradient, J its determinant and the BGM gauge enforcing the equality between original and transformed displacements, namely $\mathbf{u}(\mathbf{x})=\mathbf{U}(\mathbf{X})$, has been adopted. The transformed elasticity tensor $\mathbf{c}$ and mass density ρ can be extracted and read

$$c_{ijkl}=\frac{F_{jm}F_{ln}C_{imkn}}{J},\quad \rho=\frac{R}{J}. \tag{2.3}$$

Therein, it can be readily checked that when $\mathbf{C}$ has the minor symmetries, $\mathbf{c}$ does not. That is, $C_{ijkl}=C_{jikl}=C_{ijlk}$ does not imply a similar relation for $\mathbf{c}$. Consequently, the stress $\boldsymbol{\sigma}$ that reigns in $\{\mathbf{x}\}$ in the presence of a displacement gradient $\mathbf{e}=\boldsymbol{\nabla}\mathbf{u}$ is given by

$$\boldsymbol{\sigma}=\mathbf{c}\mathbf{e}\quad\text{or}\quad\sigma_{ij}=c_{ijkl}e_{kl} \tag{2.4}$$

and is asymmetric in general: $\sigma_{ij}\neq\sigma_{ji}$.

For our cloaking purposes, we take $\{\mathbf{x}\}$ to be a two-dimensional elastic medium composed of three regions (figure 1*c*). The central region $\{\|\mathbf{x}\|<r_i\}$ is an inclusion with arbitrary elasticity tensor $\mathbf{c}(\mathbf{x})$. The outer region $\{\|\mathbf{x}\|>r_c\}$ is the background medium, assumed isotropic with a Lamé pair (λ,μ) and mass density R. The remaining ring $\{r_i<\|\mathbf{x}\|<r_c\}$ is an axisymmetric coating of thickness r_c-r_i fulfilling the function of a cloak. Its constitutive relation is determined thanks to equation (2.3) once $\boldsymbol{\phi}$ has been specified to the blow-up transformation of figure 1. Following Brun *et al.* [12], that relation reads

$$\begin{bmatrix}\sigma_{11}\\ \sigma_{22}\\ \sigma_{12}\\ \sigma_{21}\end{bmatrix}=\begin{bmatrix}(2\mu+\lambda)f & \lambda_o & 0 & 0\\ \lambda & \dfrac{(2\mu+\lambda)}{f} & 0 & 0\\ 0 & 0 & \dfrac{\mu}{f} & \mu\\ 0 & 0 & \mu & \mu f\end{bmatrix}\begin{bmatrix}e_{11}\\ e_{22}\\ e_{12}\\ e_{21}\end{bmatrix},\quad f=\frac{\|\mathbf{x}\|-r_i}{\|\mathbf{x}\|}, \tag{2.5}$$

where components have been calculated in the normalized polar basis $(\mathbf{m},\mathbf{n})$ with $\mathbf{m}=\mathbf{x}/\|\mathbf{x}\|$. Finally, the mass density of the cloak is

$$\rho=\frac{r_c^2}{(r_c-r_i)^2}fR. \tag{2.6}$$

The major obstacle facing elastic cloaking is to design elastic materials whose behaviour is described by the two foregoing relations (2.5) and (2.6).

(b) Design heuristics: why degenerate polar lattices are necessary

There are three insights that can guide our efforts in designing cloaking materials. These are presented and discussed next.

The first insight is that a material where the minor symmetries are broken is necessarily a *polar* material, i.e. a material that elastically resists rotations. At the same time, a polar material is a material submitted to a distribution of restoring body torques. To see that, let $\mathbf{c}$ be an elasticity tensor lacking the minor symmetries, e.g. with $c_{1212}\neq c_{1221}$. Then let $\mathbf{u}$ describe an infinitesimal plane rotation of angle θ. Accordingly, the displacement gradient $\mathbf{e}$ is skewsymmetric with $e_{11}=e_{22}=0$ and $e_{21}=-e_{12}=\theta$. In that case, the shear stresses $\sigma_{12}=(c_{1221}-c_{1212})\theta$ and $\sigma_{21}=(c_{2121}-c_{2112})\theta$ are non-zero meaning that the material is indeed polar. Furthermore, the difference

between the shear stresses $\sigma_{12}-\sigma_{21}=(2c_{1221}-c_{1212}-c_{2121})\theta$ is also non-zero and directly quantifies the restoring body torques that emerge as a response to a rotation by an angle θ.

The second insight is rank conservation: seen as linear maps, $\mathbf{C}$ and $\mathbf{c}$ have the same rank $d(d+1)/2$ in dimension d. Therefore, they have an equal number of zero modes, namely $d(d-1)/2$. That is, for each tensor $\mathbf{E}$ such that $\mathbf{CE}=\mathbf{0}$, there exists a tensor $\mathbf{e}=\mathbf{EF}^{-1}$ such that $\mathbf{ce}=\mathbf{0}$. If the original material is a classical one, then the only zero modes it admits are rotations meaning that all the $\mathbf{E}$s are skewsymmetric. But then, owing to the multiplication by $\mathbf{F}^{-1}$, $\mathbf{e}$ is no longer skewsymmetric. That is, the transformed material admits zero modes that are not rotations; it is *degenerate*. Therefore, the cloak's material must exhibit a high volume fractions of void, as in foams or lattice materials, so as to stretch or shear under zero stress. In the present case with $d=2$, $\mathbf{c}$ is of rank 3 and admits a unique zero mode. This can be checked through relation (2.5). As a matter of fact, $\mathbf{e}_{\mathrm{zm}}=f\mathbf{m}\otimes\mathbf{n}-\mathbf{n}\otimes\mathbf{m}$ satisfies $\mathbf{ce}_{\mathrm{zm}}=\mathbf{0}$.

The third and last insight is particular to isotropic backgrounds. It consists in observing that the principal directions of $\mathbf{F}$ yield planes of mirror symmetry.

In conclusion, with an isotropic background in two dimensions, it is necessary that our lattice design of an elastic cloak (*i*) feature distributed restoring body torques, (*ii*) collapse effortlessly under $\mathbf{e}_{\mathrm{zm}}$ and (*iii*) be rectangular so as to exhibit two orthogonal planes of symmetry.

(c) A degenerate polar lattice cloak

Following the guidelines described above, we fill the coating ring $\{r_i<\|\mathbf{x}\|<r_c\}$ with an inhomogeneous lattice as shown in figure 2*a*. A magnified local view of the lattice is depicted in figure 2*b*. The lattice is rectangular with a unit cell containing two diagonal springs of constant α and one vertical spring of constant β. Furthermore, a unit cell contains a single mass m submitted to a restoring torque per radian per unit cell area κ as illustrated in figure 2*c*. Finally, all contacts are assumed to be hinge-like.

Now we focus on the local elastic response of the lattice in the vicinity of position $\mathbf{x}$. Call ϵ the elastic energy per unit cell area under a uniform displacement gradient $\mathbf{e}$ of the lattice and a uniform twisting of the masses by an angle ψ. Energy ϵ is composed of three terms

$$\epsilon=\epsilon_\alpha+\epsilon_\beta+\epsilon_\kappa \tag{2.7}$$

corresponding to the energy stored in the springs of constant α, the spring of constant β and in the grounded torsion spring of constant κ, respectively. These admit the expressions

$$\left.\begin{aligned}\epsilon_\alpha&=\frac{\alpha}{2v}[(\mathbf{er}_1+2d\psi\mathbf{m})\cdot\mathbf{m}_\theta]^2+\frac{\alpha}{2v}[(\mathbf{er}_2+2d\psi\mathbf{m})\cdot\mathbf{m}'_\theta]^2\\ \text{and}\qquad\epsilon_\beta&=\frac{\beta}{2v}(\mathbf{er}_3\cdot\mathbf{n})^2,\quad \epsilon_\kappa=\frac{\kappa}{2}\psi^2,\end{aligned}\right\} \tag{2.8}$$

where $v=ab/2$ is the unit cell area, $d=(bc-as)/(4c)$ is half the length of a mass, $\mathbf{r}_1=a\mathbf{m}/2+b\mathbf{n}/2$, $\mathbf{r}_2=-a\mathbf{m}/2+b\mathbf{n}/2$ and $\mathbf{r}_3=-b\mathbf{n}$ are lattice vectors, and where $\mathbf{m}_\theta=c\mathbf{m}+s\mathbf{n}$ and $\mathbf{m}'_\theta=-c\mathbf{m}+s\mathbf{n}$ are unit vectors with $c\equiv\cos\theta$ and $s\equiv\sin\theta$.

At equilibrium, ψ is such that ϵ is at its minimum characterized by

$$\frac{\partial\epsilon}{\partial\psi}=0, \tag{2.9}$$

or equivalently,

$$2cd\alpha(\mathbf{er}_1\cdot\mathbf{m}_\theta+2cd\psi)-2cd\alpha(\mathbf{er}_2\cdot\mathbf{m}'_\theta-2cd\psi)+v\kappa\psi=0. \tag{2.10}$$

This leads to a new expression of ϵ as a function of $\mathbf{e}$ alone and where ψ can be expressed as

$$\psi=-2cd\alpha\frac{ase_{21}+bce_{12}}{8c^2d^2\alpha+v\kappa}. \tag{2.11}$$

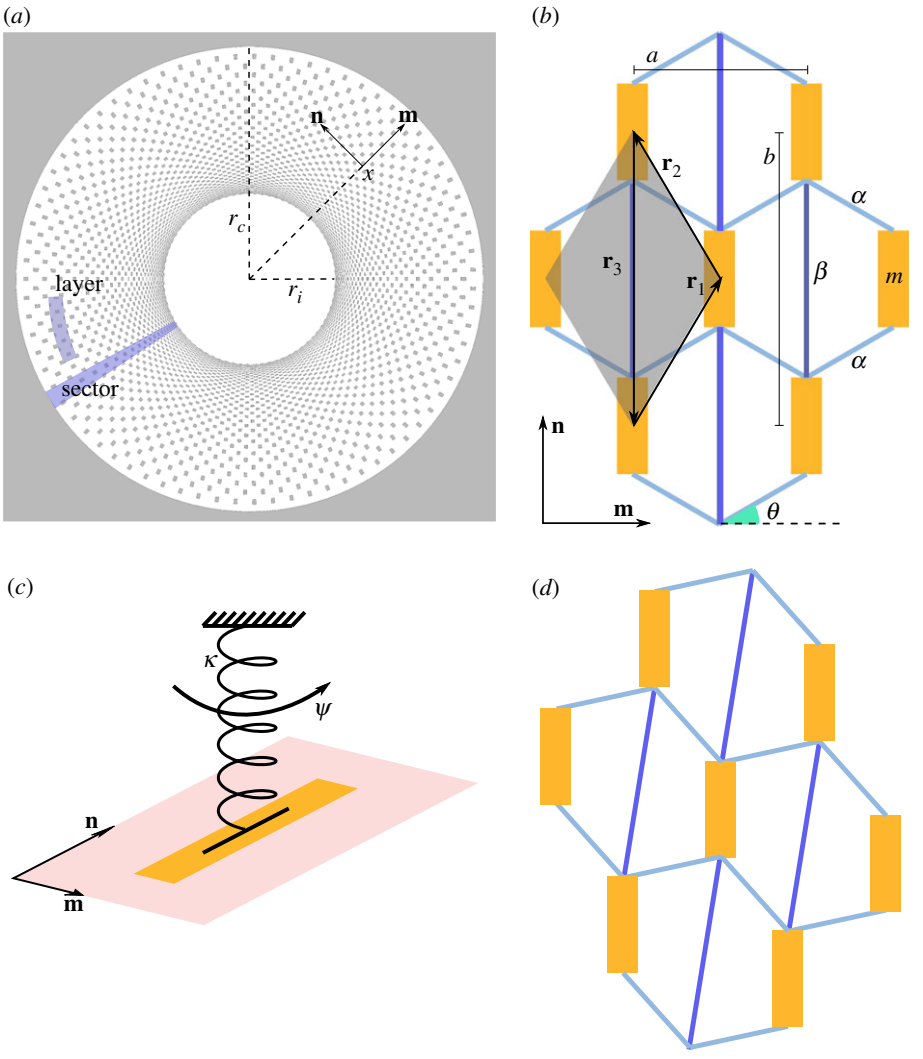

Figure 2. A two-dimensional lattice elastic cloak. (*a*) Cloak geometry: the inclusion is a void coated by a lattice and embedded in an isotropic background; the bonds of the lattice are not depicted. (*b*) Local lattice geometry at position **x**: rectangles are rigid masses submitted to a restoring torque; edges are springs; all contacts are hinge-like. (*c*) A mechanism by which restoring torques can be applied. (*d*) The configuration of the lattice under the action of the zero mode $\mathbf{e}_{\mathrm{zm}}$. (Online version in colour.)

The lattice's Hooke's Law $\boldsymbol{\sigma} = \partial\epsilon/\partial\mathbf{e}$ follows immediately and reads

$$\begin{bmatrix} \sigma_{11} \\ \sigma_{22} \\ \sigma_{12} \\ \sigma_{21} \end{bmatrix} = \begin{bmatrix} \dfrac{ac^2\alpha}{b} & cs\alpha & 0 & 0 \\ cs\alpha & \dfrac{b(\alpha s^2 + 2\beta)}{a} & 0 & 0 \\ 0 & 0 & \dfrac{b^2c^2\alpha\kappa}{\alpha(bc-as)^2 + ab\kappa} & \dfrac{abcs\alpha\kappa}{\alpha(bc-as)^2 + ab\kappa} \\ 0 & 0 & \dfrac{abcs\alpha\kappa}{\alpha(bc-as)^2 + ab\kappa} & \dfrac{a^2s^2\alpha\kappa}{\alpha(bc-as)^2 + ab\kappa} \end{bmatrix} \begin{bmatrix} e_{11} \\ e_{22} \\ e_{12} \\ e_{21} \end{bmatrix}. \tag{2.12}$$

Last, it is worth mentioning that the suggested lattice is polar as it features an asymmetric stress and is degenerate as it admits a zero mode of the form $\mathbf{e}_{\mathrm{zm}} = (as/bc)\mathbf{m} \otimes \mathbf{n} - \mathbf{n} \otimes \mathbf{m}$. The action of the zero mode on the lattice is exemplified in figure 2*d*.

(d) Parameters identification

A straightforward comparison between the lattice's Hooke's Law (2.12) and that of the cloak (2.5) reveals that they match if the parameters $(\alpha, \beta, \kappa, \theta, a/b)$ are chosen to satisfy

$$f = \frac{as}{bc}, \quad \lambda = cs\alpha, \quad \mu = \frac{abcs\alpha\kappa}{\alpha(bc - as)^2 + ab\kappa}, \tag{2.13}$$

but also

$$2\frac{\mu}{\lambda} + 1 = \frac{c^2}{s^2} = \frac{s^2 + 2\beta/\alpha}{c^2} = \frac{2ab\kappa}{\alpha(bc - as)^2 + ab\kappa} + 1. \tag{2.14}$$

Solving these relations yields the local design parameters of a lattice fulfilling the function of a cloak, namely

$$\left.\begin{aligned} \kappa &= \frac{\lambda\mu}{\lambda - \mu}\frac{(1-f)^2}{f}, \\ \theta &= \arctan\sqrt{\frac{\lambda}{2\mu + \lambda}} \in (0, \pi/2), \\ \alpha &= 2(\mu + \lambda)\sqrt{\frac{\lambda}{2\mu + \lambda}}, \\ \beta &= \frac{(2\mu + \lambda)^2 - \lambda^2}{2\sqrt{\lambda}\sqrt{2\mu + \lambda}} > 0 \\ \text{and} \quad \frac{a}{b} &= f\sqrt{\frac{2\mu + \lambda}{\lambda}}. \end{aligned}\right\} \tag{2.15}$$

As for mass, it is given by

$$m = \frac{ab}{2}\rho. \tag{2.16}$$

Note that the suggested design maintains the parameters θ, α and β uniform throughout the cloak whereas parameters $\kappa, a/b$ and m depend on position $\mathbf{x}$ through f. Note also that enforcing stability by rejecting torsion springs with a negative constant κ implies $\mu \leq \lambda$ and places a constraint on the isotropic backgrounds for which a lattice cloak can be designed in this manner. A generalization of our design, that would work for arbitrary anisotropic backgrounds in three dimensions, is presented in the next section.

For the example treated next, we set $\lambda = \mu$ for simplicity. Thus, the design parameters simplify into

$$\kappa \to \infty, \quad \theta = \frac{\pi}{6}, \quad \alpha = \beta = \frac{4\mu}{\sqrt{3}}, \quad \frac{a}{b} = f\sqrt{3}. \tag{2.17}$$

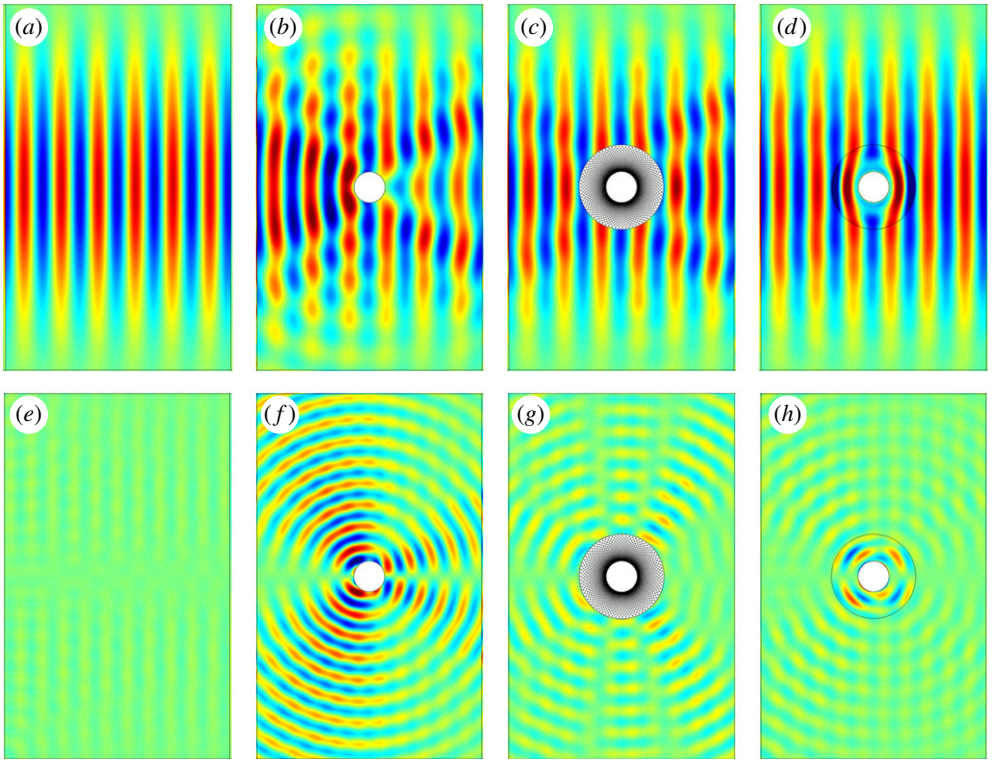

Figure 3. Normalized divergence (*a–d*) and curl (*e–h*) of the displacement field as colour maps for an incident 40 kHz plane pressure wave. Ideal cloaking should show zero curl out of the cloak's domain: residual curl can be interpreted as an error measure. Plots (*a*,*e*) correspond to the intact background medium; (*b*,*f*) to a non-coated void; (*c*,*g*) to a lattice-coated void; and (*d*,*h*) to a continuously coated void. (Online version in colour.)

In particular, κ is infinite and mass rotation is completely blocked. Then, letting N be the number of angular sectors in the coating, it comes that

$$b = \frac{2\pi\|\mathbf{x}\|}{N}, \quad a = 2\pi\sqrt{3}\frac{\|\mathbf{x}\| - r_i}{N}, \quad m = \frac{2\pi^2\sqrt{3}}{N^2}r_c^2\left(\frac{\|\mathbf{x}\| - r_i}{r_c - r_i}\right)^2 R. \tag{2.18}$$

As for the number of layers M, it is infinite in theory so as to permit $\|\mathbf{x}\|$ to reach the inner radius r_i. In practice, M is chosen large and $\|\mathbf{x}\|$ reaches a minimum $r_i' > r_i$. Cloaking is, therefore, approximate in practice but becomes ideal in the theoretical limit $M, N \to \infty$ as $r_i' \to r_i$.

(e) Cloaking simulations

In the following numerical simulations, the plane stress hypothesis was adopted. We cloak a void of radius $r_i' = 55$ mm with a coating of radius $r_c = 150$ mm embedded in a rectangular plate of 1mm thickness and of inplane Lamé parameters $\lambda = \mu = 2.5 \times 10^6$ Pa × m and mass density $R = 2.7\,\mathrm{kg\,m^{-2}}$ (figure 2*a*). The lattice cloak consists of $M = 22$ layers and $N = 75$ sectors and has a theoretical inner radius of $r_i = 50$ mm. Navier's equations in the background medium coupled to Newton's equations in the coating were solved using the finite-element method and with the help of the commercial software COMSOL Multiphysics. Each mass in the cloak's domain is modelled as a solid medium of sufficiently large modulus. Furthermore, its nodes are constrained to have equal displacements so as to block rotations. Last, springs are modelled as pairs of point forces depending on nodal displacements.

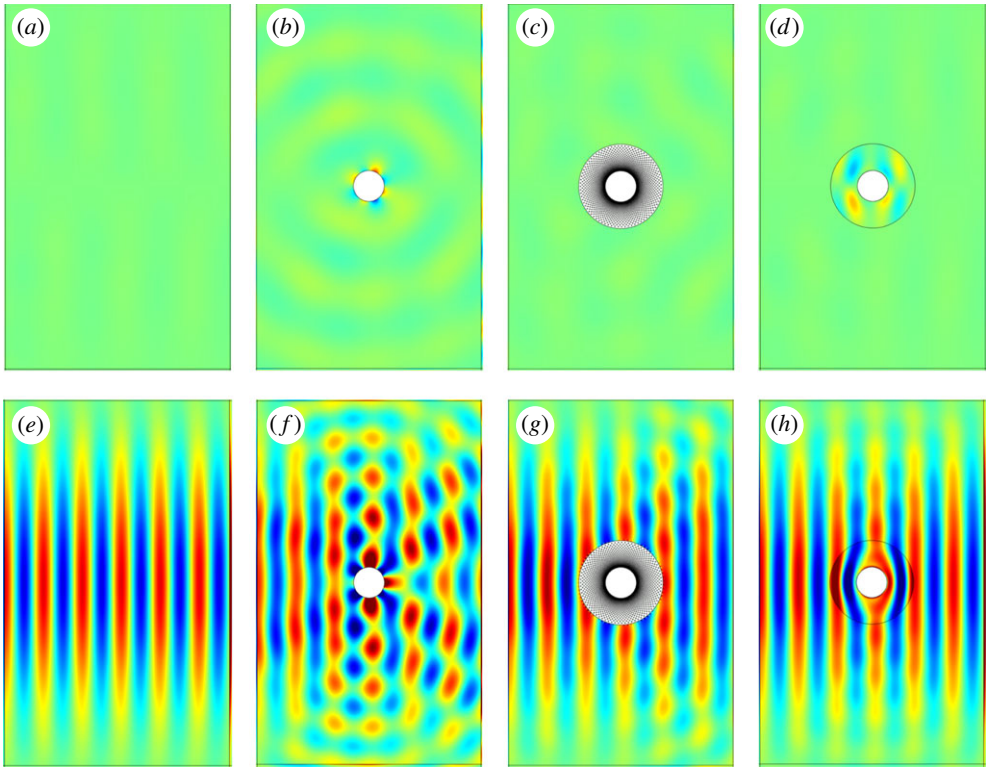

Figure 4. Normalized divergence (*a–d*) and curl (*e–h*) of the displacement field as colour maps for an incident 22 kHz plane shear wave. Ideal cloaking should show zero divergence out of the cloak's domain: residual divergence can be interpreted as an error measure. Plots (*a*,*e*) correspond to the intact background medium; (*b*,*f*) to a non-coated void; (*c*,*g*) to a lattice-coated void; and (*d*,*h*) to a continuously coated void. (Online version in colour.)

Given linearity and isotropy, it is sufficient to characterize the cloak's behaviour in three configurations: under an incident plane harmonic pressure wave, under an incident plane harmonic shear wave and under uniaxial static compression. In the dynamic regime, incident waves with Gaussian profiles are emitted from the left boundary of the simulation domain and perfectly matched layers are appended to all sides so as to eliminate reflections. Note that reflections would not jeopardize the cloak's performance but constitute a nuisance for the interpretation of the results. In the static regime, uniform normal displacements are applied to the left and right boundaries while leaving the top and bottom boundaries free of normal stresses.

Results are shown in figures 3–5 for an incident pressure wave, incident shear wave and for unidirectional compression, respectively. For reference, we carried out the same simulations where the background medium is intact (plots *a* and *e*); where the void is non-coated (*b* and *f*); where the void is lattice-coated (*c* and *g*); and in the homogenization limit where the discrete cloak is substituted by a fictitious continuous material of the same behaviour (*d* and *h*). Therein, the real part of the divergence and curl of the displacement field is shown as a colour map over continuous domains but is not available over discrete regions *a priori* and these are left uncoloured. Most importantly, beyond the cloak's domain, whenever the divergence or the curl component is dominant over the other, the secondary component can be interpreted as an error or a scattering measure.

Comparing plots (*b*,*f*) to (*c*,*g*), respectively, it is seen that the lattice cloak manages to suppress the scattering, or strain localization, by or around the void to a high and satisfactory degree although without being perfect. The cloaking error, e.g. the residual scattering, has two sources: first, by comparing plots (*c*,*g*) to (*d*,*h*), it is seen that the lattice is not operating yet

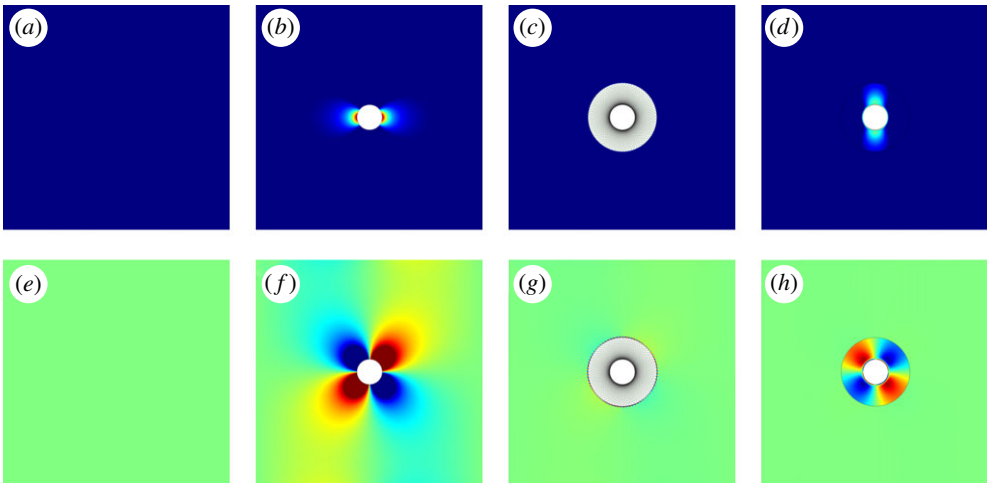

Figure 5. Normalized divergence (*a–d*) and curl (*e–h*) of the displacement field as colour maps under horizontal compression. Ideal cloaking should show zero curl out of the cloak's domain: residual curl can be interpreted as an error measure. Plots (*a*,*e*) correspond to the intact background medium; (*b*,*f*) to a non-coated void; (*c*,*g*) to a lattice-coated void; and (*d*,*h*) to a continuously coated void. (Online version in colour.)

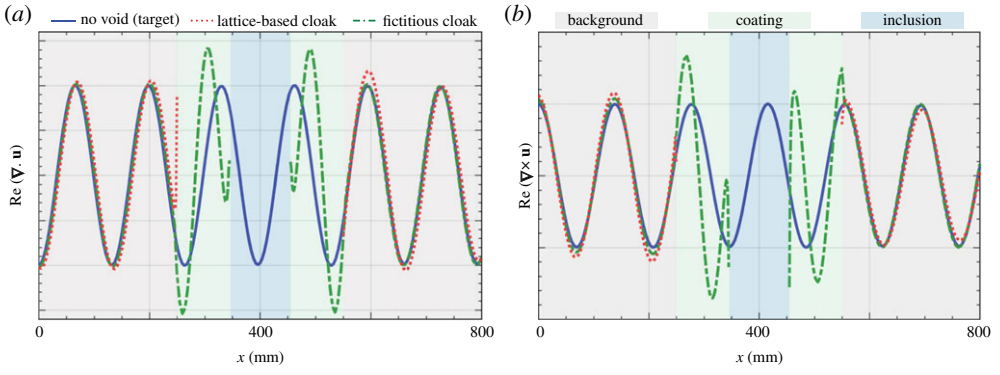

Figure 6. Normalized divergence (*a*) and curl (*b*) of the displacement field as a function of position *x* along the midspan of the simulation domain, respectively, for the configurations of figure 3*a*,*c*,*d* and for the configurations of figure 4*a*,*c*,*d*. (Online version in colour.)

in the homogenization limit; second, by comparing plots (*a*,*e*) to (*d*,*h*), it is seen that even the homogenization limit does not show perfect cloaking due to the inner radius r_i' being slightly larger than the theoretical value r_i. The remedy to both sources of error is an increase in the number of layers and sectors N and M. This analysis is further confirmed by the fact that the performance of the cloak is visibly better in statics than in dynamics, that is when wavelengths are larger compared to the unit cell parameters.

To consolidate our results quantitatively, the fields in figure 3*a*,*c*,*d* are plotted against position x along the midspan of the simulation domain. The normalized profiles are depicted in figure 6*a*. It is seen that over the background medium, all three profiles match well overall. Remarkably, the most significant surge of error occurs at the boundary of the cloak at $x = 250$ mm but then dies exponentially fast as x moves into the bulk of the background. Consequently, at that interface, where the discrete domain of the lattice cloak meets the continuous domain of the background, evanescent fields emerge. These are similar to the evanescent fields that appear in a halfspace as a result to a point force being applied to its free boundary. As M and N grow, the number of point

forces applied to the background increases and the spacing between their points of application decreases. In the limit $M, N \to \infty$, the point forces converge toward a smoothly distributed load and the parasitic evanescent fields disappear as a result; only then our lattice cloak becomes perfect. Figure 6*b* shows the normalized profile of the fields of figure 4*e*,*c*,*d* as a function of x. Similar observations hold in that case.

3. A generalization to anisotropic backgrounds in three dimensions

The lattice cloak of the previous section is specific to two-dimensional isotropic backgrounds. Furthermore, if only positive torsion spring constants κ are permitted, then the background must satisfy $\mu \leq \lambda$. Here, we prove that lattice designs of cloaks exist in three dimensions for arbitrary anisotropic backgrounds. More generally, we construct lattice materials whose behaviour is form-invariant under the BGM gauge. The proof closely follows Milton & Cherkaev's [28] construction of arbitrary elastic solids as mixtures of pentamode materials. First, the approach is motivated thanks to a spectral decomposition of the elasticity tensor. Second, we modify Milton and Cherkaev's pentamodes so as to enable access to elasticity tensors without the minor symmetries. These modified pentamodes are lattice materials that can support a unique stress state, be it symmetric or not, and are renamed 'rank-1 materials'. Finally, we conclude that mixtures of rank-1 materials can exhibit any elasticity tensor with or without the minor symmetries.

(a) Spectral decomposition and definitions

Once transformed, the elasticity tensor $\mathbf{c}$ loses the minor symmetries. Fortunately, $\mathbf{c}$ still has major symmetry and remains non-negative. Hence, it can be decomposed into a sum of projectors

$$\mathbf{c} = \sum_{s=1}^{d^2} \mathbf{c}_s = \sum_{s=1}^{d^2} \mu_s \boldsymbol{\tau}_s \otimes \boldsymbol{\tau}_s, \tag{3.1}$$

where the μ_s are non-negative elastic moduli and the $\boldsymbol{\tau}_s$ are orthonormal eigentensors such that $\mathbf{c}\boldsymbol{\tau}_s = \mu_s \boldsymbol{\tau}_s$ and $\boldsymbol{\tau}_s \cdot \boldsymbol{\tau}_{s'} = \delta_{ss'}$. Note that since $\mathbf{c}$ does not obey the minor symmetries, there exists at least one asymmetric $\boldsymbol{\tau}_s$. Conversely, if all $\boldsymbol{\tau}_s$ are symmetric, then $\mathbf{c}$ has the minor symmetries.

A material whose elasticity tensor is equal to one of the $\mathbf{c}_s$ is called a rank-1 material. Such a material can support a unique stress state proportional to $\boldsymbol{\tau}_s$ and collapses effortlessly under any gradient $\mathbf{e}$ that is orthogonal to $\boldsymbol{\tau}_s$. As a matter of fact, $\boldsymbol{\tau}_s \cdot \mathbf{e} = \mathbf{0}$ implies $\mathbf{c}_s\mathbf{e} = \mathbf{0}$. More generally, a rank-n material is one capable of supporting exactly n linearly independent stress states while collapsing under all gradients orthogonal to these states. Note that a material is of rank n if and only if its elasticity tensor $\mathbf{c}$ is of rank n when seen as a linear map over the space of second-order tensors.

With this definition, recall that a classical elastic solid in dimension d is of rank $d(d+1)/2$ since it supports d traction/compression states and $d(d-1)/2$ shear states while 'collapsing' under $d(d-1)/2$ rotations. As changes of coordinates preserve ranks, the possibility for a full theory of transformation elasticity under the BGM gauge hinges on designing arbitrary non-negative elasticity tensors of rank $d(d+1)/2$ with major symmetry and with or without the minor symmetries.

Hereafter, we closely follow Milton and Cherkaev and design a material with elasticity tensor $\mathbf{c}$ in two steps. First, we build rank-1 materials whose elasticity tensors are equal to the individual $\mathbf{c}_s$. Second, we mix these building blocks into a single material whose elasticity tensor is equal to $\mathbf{c}$.

(b) Design of rank-1 materials

Consider the lattice whose unit cell is depicted in figure 7. A unit cell is composed of a single rigid mass placed at the origin of the coordinate system and connected to $d+1$ vertices placed at the tips of vectors $\mathbf{r}_j$. The connections are spring-like with constants k_j and are directed along

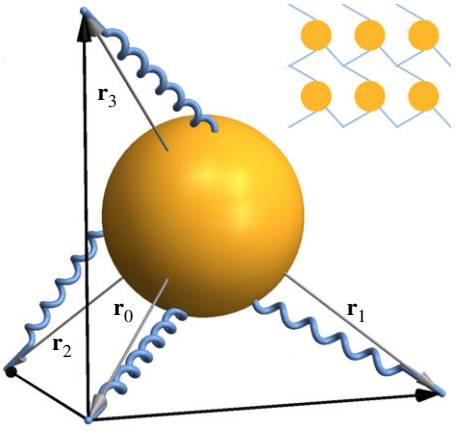

Figure 7. The unit cell of a rank-1 material: black arrows are lattice vectors; vectors $\mathbf{r}_j$ are in grey; vectors $\mathbf{s}_j$ (not shown) are directed along the coils; all contacts (coil–coil and coil-sphere) behave like hinges; coils behave like linear springs; spheres have a fixed absolute orientation but are free to translate. When the $\mathbf{r}_j$ are parallel to the coils, the lattice becomes equivalent to a Milton and Cherkaev's pentamode. The inset shows a two-dimensional representation of the lattice. (Online version in colour.)

the unitary vectors $\mathbf{s}_j$; note that the $\mathbf{s}_j$ and $\mathbf{r}_j$ are not necessarily aligned. A mass originally has $d(d+1)/2$ degrees of freedom corresponding to rigid body motions. However, we assume each mass to be submitted to $d(d-1)/2$ restoring torques sufficiently strong to block rotations while leaving free the d degrees of freedom of translational motion. Accordingly, the elastic energy density within one unit cell of volume v submitted to a displacement gradient $\mathbf{e}$ is

$$\epsilon = \frac{1}{2v}\sum_{j=0}^{d} k_j[\mathbf{s}_j \cdot (\mathbf{e}\mathbf{r}_j - \boldsymbol{\delta})]^2, \tag{3.2}$$

where $\mathbf{e}\mathbf{r}_j$ is the imposed displacement of vertex j and $\boldsymbol{\delta}$ is the displacement of the mass. Hence, $\mathbf{s}_j \cdot (\mathbf{e}\mathbf{r}_j - \boldsymbol{\delta})$ is the elongation of spring j and the expression of ϵ follows. At equilibrium, $\boldsymbol{\delta}$ is such that ϵ is equal to its minimum characterized by

$$\frac{\partial \epsilon}{\partial \boldsymbol{\delta}} = \mathbf{0}, \tag{3.3}$$

or equivalently

$$\sum_{j=0}^{d} k_j[\mathbf{s}_j \cdot (\mathbf{e}\mathbf{r}_j - \boldsymbol{\delta})]\mathbf{s}_j = \mathbf{0}. \tag{3.4}$$

The $\mathbf{s}_j$ being $d+1$ vectors in d dimensions, there exist scalars x_j, $j = 0 \ldots d$, such that

$$\sum_{j=0}^{d} x_j \mathbf{s}_j = \mathbf{0}. \tag{3.5}$$

Comparing (3.4) and (3.5), it comes that

$$k_j \mathbf{s}_j \cdot (\mathbf{e}\mathbf{r}_j - \boldsymbol{\delta}) = \gamma x_j, \tag{3.6}$$

where γ is a j-independent similarity ratio. Multiplying by x_j/k_j and summing over j then yields

$$\sum_{j=0}^{d} x_j \mathbf{s}_j \cdot \mathbf{e}\mathbf{r}_j = \gamma \sum_{k=0}^{d} \frac{x_j^2}{k_j} \tag{3.7}$$

or

$$\gamma = \frac{\boldsymbol{\tau}^{\mathrm{lat}} \cdot \mathbf{e}}{\sum_{k=0}^{d} x_j^2/k_j}; \quad \boldsymbol{\tau}^{\mathrm{lat}} = \sum_{j=0}^{d} x_j \mathbf{s}_j \otimes \mathbf{r}_j. \tag{3.8}$$

Now, combining (3.2), (3.6) and (3.8), we deduce that the elastic energy in fact depends on a unique scalar, namely $\boldsymbol{\tau}^{\mathrm{lat}} \cdot \mathbf{e}$, through

$$\epsilon = \frac{(\boldsymbol{\tau}^{\mathrm{lat}} \cdot \mathbf{e})^2}{2v \sum_j x_j^2/k_j}. \tag{3.9}$$

The lattice is, therefore, clearly of rank 1: for any strain $\mathbf{e}$ orthogonal to tensor $\boldsymbol{\tau}^{\mathrm{lat}}$, the scalar product $\boldsymbol{\tau}^{\mathrm{lat}} \cdot \mathbf{e}$ vanishes and so does ϵ. Conversely, the unique stress state that the lattice is capable of supporting is given by tensor $\boldsymbol{\tau}^{\mathrm{lat}}$. This can also be seen by deriving the expression of the effective elasticity tensor. We find

$$\mathbf{c}^{\mathrm{lat}} = \frac{\partial^2 \epsilon}{\partial \mathbf{e} \partial \mathbf{e}} = \frac{1}{v \sum_j x_j^2/k_j} \boldsymbol{\tau}^{\mathrm{lat}} \otimes \boldsymbol{\tau}^{\mathrm{lat}} \tag{3.10}$$

is a dyadic product and is of rank 1.

In conclusion of this subsection, as long as the vectors $\mathbf{r}_j$ and $\mathbf{s}_j$ are misaligned, the stress $\boldsymbol{\tau}^{\mathrm{lat}}$ will be asymmetric and $\mathbf{c}^{\mathrm{lat}}$ will lack the minor symmetries. When the $\mathbf{r}_j$ and the $\mathbf{s}_j$ are aligned, the rank-1 material becomes identical to a Milton and Cherkaev's pentamode. In any case, by appropriately choosing vectors $\mathbf{r}_j$ and $\mathbf{s}_j$, it is possible to target any single eigentensor $\boldsymbol{\tau}_s$ and subsequently any single elasticity tensor $\mathbf{c}_s$. We refer to Milton and Cherkaev's original paper for more details regarding this assertion.

(c) Design of rank-*n* materials

Now take two weakly interacting interpenetrated lattices with elasticity tensors $\mathbf{c}_s$ and $\mathbf{c}_{s'}$. Applying a displacement gradient $\mathbf{e}$ will generate an energy $\mu_{s,s'}(\boldsymbol{\tau}_{s,s'} \cdot \mathbf{e})^2/2$ in the first and second lattice, respectively. Accordingly, the elasticity tensor of the mixture is simply $\mathbf{c}_s + \mathbf{c}_{s'}$. Iterating the process and mixing up to d^2 lattices, all non-negative elasticity tensors $\mathbf{c}$ satisfying major symmetry can be generated. This concludes our proof that the set of elastic materials submitted to restoring torques is invariant by transformations under the BGM gauge.

4. Conclusion

In conclusion, full transformation elasticity and cloaking, in particular, have been proved possible in principle thanks to a class of degenerate polar lattices that elastically resist rotations while admitting a set of collapse mechanisms. In two dimensions, the proposed lattice exhibits a rank-3 elasticity tensor lacking the minor symmetries as required by the transformation method under the BGM gauge. The lattice cloak was numerically tested under various static and dynamic loadings and showed satisfactory performance.

Experimental demonstrations are much desired but face two challenges. The first is to devise a practical way of imposing the required torques. The second is to reduce the number of sectors and layers in the cloak as much as possible. This would contradict the homogenization limit however and an optimal trade-off is to be found. In doing so, it could be beneficial to investigate better ways to connect the background continuum to the discrete domain of the cloak and to take into account the jumps occurring at that interface so as to eliminate any parasitic evanescent fields. As for the restoring torques, they can be applied in practice thanks to grounded torsion springs. If external intervention is prohibited or deemed disadvantageous, effective restoring torques can be dynamically applied by embedding a rotational resonator within each mass. In that case, our results must be restated as they become valid at single non-zero frequencies in the harmonic regime, thus excluding statics. Future efforts tackling these issues are most welcome.

Data accessibility. The paper has no experimental data.

Authors' contributions. H.N. and G.L.H. conceived the concept and model. H.N. designed the lattices and derived the governing equations. Y.Y.C. built the numerical model and performed the simulations. G.L.H. interpreted the results and supervised the research. All authors gave final approval for publication.

Competing interests. The authors have no competing interests.

Funding. This work is supported by the Army Research office under grant no. W911NF-18-1-0031 with Program Manager Dr David M. Stepp.

References

1. Hu J, Zhou X, Hu G. 2009 Design method for electromagnetic cloak with arbitrary shapes based on Laplace's equation. *Opt. Express* **17**, 1308–1320. (doi:10.1364/OE.17.001308)
2. Greenleaf A, Lassas M, Uhlmann G. 2003 Anisotropic conductivities that cannot be detected by EIT. *Physiol. Meas.* **24**, 413–419. (doi:10.1088/0967-3334/24/2/353)
3. Greenleaf A, Lassas M, Uhlmann G. 2003 On nonuniqueness for Calderón's inverse problem. *Math. Res. Lett.* **10**, 685–693. (doi:10.4310/MRL.2003.v10.n5.a11)
4. Leonhardt U. 2006 Optical conformal mapping. *Science* **312**, 1777–1780. (doi:10.1126/science.1126493)
5. Pendry JB, Schurig D, Smith DR. 2006 Controlling electromagnetic fields. *Science* **312**, 1780–1782. (doi:10.1126/science.1125907)
6. Cummer SA, Schurig D. 2007 One path to acoustic cloaking. *New J. Phys.* **9**, 45. (doi:10.1088/1367-2630/9/3/045)
7. Chen H, Chan CT. 2007 Acoustic cloaking in three dimensions using acoustic metamaterials. *Appl. Phys. Lett.* **91**, 183518. (doi:10.1063/1.2803315)
8. Norris AN. 2015 Acoustic cloaking. *Acoust. Today* **11**, 38–46.
9. Norris AN. 2008 Acoustic cloaking theory. *Proc. R. Soc. A* **464**, 2411–2434. (doi:10.1098/rspa.2008.0076)
10. Smith JD. 2011 Application of the method of asymptotic homogenization to an acoustic metafluid. *Proc. R. Soc. A* **467**, 3318–3331. (doi:10.1098/rspa.2011.0231)
11. Milton GW, Briane M, Willis JR. 2006 On cloaking for elasticity and physical equations with a transformation invariant form. *New J. Phys.* **8**, 248–267. (doi:10.1088/1367-2630/8/10/248)
12. Brun M, Guenneau S, Movchan AB. 2009 Achieving control of in-plane elastic waves. *Appl. Phys. Lett.* **94**, 061903. (doi:10.1063/1.3068491)
13. Diatta A, Guenneau S. 2014 Controlling solid elastic waves with spherical cloaks. *Appl. Phys. Lett.* **105**, 021901. (doi:10.1063/1.4887454)
14. Norris AN, Shuvalov AL. 2011 Elastic cloaking theory. *Wave Motion* **48**, 525–538. (doi:10.1016/j.wavemoti.2011.03.002)
15. Farhat M, Guenneau S, Enoch S. 2009 Ultrabroadband elastic cloaking in thin plates. *Phys. Rev. Lett.* **103**, 024301. (doi:10.1103/PhysRevLett.103.024301)
16. Farhat M, Guenneau S, Enoch S, Movchan AB. 2009 Cloaking bending waves propagating in thin elastic plates. *Phys. Rev. B - Condens. Matter Mater. Phys.* **79**, 033102. (doi:10.1103/PhysRevB.79.033102)
17. Farhat M, Guenneau S, Enoch S. 2012 Broadband cloaking of bending waves via homogenization of multiply perforated radially symmetric and isotropic thin elastic plates. *Phys. Rev. B - Condens. Matter Mater. Phys.* **85**, 020301. (doi:10.1103/PhysRevB.85.020301)
18. Stenger N, Wilhelm M, Wegener M. 2012 Experiments on elastic cloaking in thin plates. *Phys. Rev. Lett.* **108**, 014301. (doi:10.1103/PhysRevLett.108.014301)
19. Brun M, Colquitt DJ, Jones IS, Movchan AB, Movchan NV. 2014 Transformation cloaking and radial approximations for flexural waves in elastic plates. *New J. Phys.* **16**, 093020. (doi:10.1088/1367-2630/16/9/093020)
20. Colquitt DJ, Brun M, Gei M, Movchan AB, Movchan NV, Jones IS. 2014 Transformation elastodynamics and cloaking for flexural waves. *J. Mech. Phys. Solids* **72**, 131–143. (doi:10.1016/j.jmps.2014.07.014)
21. Chen YY, Hu J, Huang GL. 2016 A design of active elastic metamaterials for control of flexural waves using the transformation method. *J. Intell. Mater. Syst. Struct.* **27**, 1337–1347. (doi:10.1177/1045389X15590273)
22. Parnell WJ, Norris AN, Shearer T. 2012 Employing pre-stress to generate finite cloaks for antiplane elastic waves. *Appl. Phys. Lett.* **100**, 171907. (doi:10.1063/1.4704566)

23. Parnell WJ. 2012 Nonlinear pre-stress for cloaking from antiplane elastic waves. *Proc. R. Soc. A* **468**, 563–580. (doi:10.1098/rspa.2011.0477)
24. Norris AN, Parnell WJ. 2012 Hyperelastic cloaking theory : transformation elasticity with pre-stressed solids. *Proc. R. Soc. A* **468**, 2881–2903. (doi:10.1098/rspa.2012.0123)
25. Bückmann T, Kadic M, Schittny R, Wegener M. 2015 Mechanical cloak design by direct lattice transformation. *Proc. Natl Acad. Sci. USA* **112**, 4930–4934. (doi:10.1073/pnas.1501240112)
26. Sklan SR, Pak R, Li B. 2018 Seismic invisibility: elastic wave cloaking via symmetrized transformation media. *New J. Phys.* **20**, 063013. (doi:10.1088/1367-2630/aac7ab)
27. Milton GW. 2002 *The theory of composites*. Cambridge, UK: Cambridge University Press.
28. Milton GW, Cherkaev AV. 1995 Which elasticity tensors are realizable? *J. Eng. Mater. Technol.* **117**, 483–493. (doi:10.1115/1.2804743)
29. Guevara Vasquez F, Milton GW, Onofrei D, Seppecher P. 2012 Transformation elastodynamics and active exterior acoustic cloaking. In *Acoustic metamaterials: negative refraction, imaging, lensing and cloaking* (eds RV Craster, S Guenneau), pp. 289–318. Springer Series in Materials Science. Dordrecht, The Netherlands: Springer.